# A Pharmacodynamic Study of Docetaxel in Combination with the P-glycoprotein Antagonist, Tariquidar (XR9576) in Patients with Lung, Ovarian, and Cervical Cancer

**Ronan J. Kelly**[1], **Deborah Draper**[1], **Clara C. Chen**[2], **Robert W. Robey**[1], **William D. Figg**[1], **Richard L. Piekarz**[1], **Xiaohong Chen**[1], **Erin R. Gardner**[3], **Frank M. Balis**[4], **Aradhana M. Venkatesan**[5], **Seth M. Steinberg**[6], **Tito Fojo**[1], and **Susan E. Bates**[1]

[1]Medical Oncology Branch, Center for Cancer Research, Warren G. Magnuson Clinical Center, NIH, Bethesda, MD

[2]Department of Nuclear Medicine and Radiology, Warren G. Magnuson Clinical Center, NIH, Bethesda, MD

[3]Department of Clinical Pharmacology Program, SAIC-Frederick, NCI-Frederick, MD 21702

[4]Department of Center for Childhood Cancer Research, Children's Hospital of Philadelphia, Philadelphia PA

[5]Department of Radiology and Imaging Sciences, Clinical Center, NIH

[6]Biostatistics and Data Management Section, CCR, NCI

## Abstract

**Purpose**—P-glycoprotein (Pgp) antagonists have been difficult to develop because of complex pharmacokinetic interactions and a failure to demonstrate meaningful results. Here we report the results of a pharmacokinetic and pharmacodynamic trial using a third generation, potent, non-competitive inhibitor of Pgp, tariquidar (XR9576), in combination with docetaxel.

**Experimental Design**—In the first treatment cycle, the pharmacokinetics of docetaxel (40 mg/m$^2$) were evaluated after day 1 and day 8 doses, which were administered with or without tariquidar (150 mg). $^{99m}$Tc-sestamibi scanning and CD56+ mononuclear cell rhodamine efflux assays were performed to assess Pgp inhibition. In subsequent cycles, 75 mg/m$^2$ docetaxel was administered with 150 mg tariquidar every three weeks.

**Results**—Forty-eight patients were enrolled onto the trial. Non-hematologic grade 3/4 toxicities in 235 cycles were minimal. Tariquidar inhibited Pgp-mediated rhodamine efflux from CD56+ cells and reduced $^{99m}$Tc-sestamibi clearance from the liver. A 12 to 24% increase in sestamibi uptake in visible lesions was noted in 8 of 10 patients with lung cancer. No significant difference in docetaxel disposition was observed in pairwise comparison with and without tariquidar. Four PRs were seen (4/48); three in the non-small cell lung cancer (NSCLC) cohort, measuring 40%, 57% and 67% by RECIST and one PR in a patient with ovarian cancer.

**Conclusions**—Tariquidar is well-tolerated with less observed systemic pharmacokinetic interaction than previous Pgp antagonists. Variable effects of tariquidar on retention of sestamibi

---

in imageable lung cancers suggest that follow-up studies assessing tumor drug uptake in this patient population would be worthwhile.

## Keywords

P-glycoprotein; ABC transporter; drug resistance; sestamibi imaging; lung cancer

## Introduction

Resistance to anticancer therapy remains a major problem in the treatment of cancer, highlighted in recent years by the onset of drug resistance in tumors treated with molecularly targeted agents. Drug resistance occurs via a myriad of mechanisms – including pharmacologic resistance whereby a drug fails to be activated or is rapidly excreted or inactivated; resistance at the level of the target through loss or mutation of the target; hypoxia and cell survival mechanisms; and transport-mediated resistance due to decreased drug influx and/or increased efflux, effecting reduced intracellular drug accumulation. P-glycoprotein (Pgp), a member of the ATP-binding cassette (ABC) transporter family, is able to confer resistance to a large number of functionally and chemically distinct cytotoxic compounds. Pgp, encoded by the *MDR-1 (ABCB1)* gene, is an energy-dependent efflux pump that lowers the intracellular concentrations of many chemotherapeutic agents[1,2]. It has been hypothesized that Pgp inhibition could serve an important role in previously treated and naïve tumors over-expressing the transporter. Despite correlation of Pgp expression with poor outcome in multiple settings, this hypothesis has not been confirmed clinically.

Many early phase I/II studies attempting Pgp inhibition used first-generation, non-specific Pgp inhibitors such as verapamil, dexverapamil, tamoxifen, quinidine, and cyclosporine. Results from these studies proved disappointing and failed to demonstrate an improvement in overall drug efficacy, primarily attributed to poor potency[3]. In addition, trials included heavily pretreated patients, without documented Pgp expression in tumors. The interpretation of these early studies was further hampered by a lack of randomization to prove efficacy.

### Statement of Translational Relevance

Considerable evidence suggests that drug transporters are important in pharmacology, oral absorption, drug distribution into sanctuary sites such as the CNS, and in protection of bone marrow stem cells. Whether they are important in cancer drug resistance has not been answered; attempts to show that blocking drug efflux would improve clinical outcome have largely failed. This report presents a pharmacodynamic trial confirming that tariquidar, an inhibitor of the ATP binding cassette transporters P-glycoprotein and ABCG2, can be safely administered with docetaxel, and can increase substrate accumulation in normal tissues and in some tumors of patients with lung, ovarian, or cervical cancer. The most striking observation was the marked variability of basal uptake of surrogate radionuclide into lung tumors, with minimal to modest tarquidar effects, suggesting that the understudied and unanswered question of drug uptake and penetration in tumors remains an important one.

Second generation agents with increased potency were subsequently developed, including PSC833 (valspodar), VX-710 (biricodar) and GF120918 (elacridar)[4-7]. Data from clinical trials involving second generation agents, particularly with valspodar, were likewise disappointing. Drug-drug interactions involving CYP3A4 inhibition required cytotoxic drug dose reduction due to a decrease in chemotherapeutic drug clearance, resulting in increased exposure. Several trials demonstrated increased toxicity in the experimental arm [7-9]. These

investigations led to the development of third-generation Pgp inhibitors including tariquidar (XR 9576), zosuquidar (LY335979) and laniquidar (R101933), with increased specificity and potency, and fewer pharmacokinetic interactions[10].

Tariquidar (XR9576) is a third generation Pgp antagonist. It is an anthranilic acid based drug that potently inhibits Pgp-mediated drug efflux[11-14]. At low nanomolar concentrations, the compound restores the sensitivity of resistant human tumor cell lines to cytotoxic agents including anthracyclines, vinca alkaloids and taxanes. Its duration of action is superior to previous Pgp inhibitors, with CD56+ cells in patients showing continued inhibition up to 48 hr after administration[14,15]. Although tariquidar had minimal toxicity in early testing[14,16], two large randomized multicenter trials in lung cancer closed early due to toxicity in the experimental arms. It was therefore decided that further safety testing was warranted. The primary goal of this study was to evaluate the effects of tariquidar on docetaxel pharmacokinetics and to establish whether tariquidar at the administered dose modulates Pgp in tumors of the patients enrolled. Additional safety data were to be collected in the setting of combined therapy. Trials combining other Pgp modulators with taxanes have shown inhibition of drug clearance, requiring decreased taxane dosage[10]. In contrast, previous studies with tariquidar suggested minimal pharmacokinetic interactions with doxorubicin, paclitaxel and vinorelbine that were clinically insignificant relative to natural intra-patient variability in pharmacokinetics[14-17]. We anticipated that the docetaxel dose in the combination would not require a reduction since 75 mg/m$^2$ provided a margin of safety as a dose that is routinely used and better tolerated than the FDA approved dose of 100 mg/m$^2$ [18,19]. The pharmacokinetic portion of the study used a two period crossover design and was analyzed accordingly.

## Patients and Methods

### Patient Selection

Forty-eight patients were enrolled onto the trial, which was reviewed and approved by the National Cancer Institute's Institutional Review Board. Verbal and written consent was obtained from all patients. Enrollment criteria included age older than 18 years, an Eastern Cooperative Oncology Group (ECOG) performance status of 0-2, and a life expectancy greater than 3 months. Eligibility required histologic or cytologic confirmation of lung, cervical, or ovarian cancer, at least one prior standard treatment regimen, and no known standard therapy capable of extending life expectancy.

Suitable candidates required a platelet count $\geq$ 90,000/mL, absolute granulocyte count (AGC) $\geq$ 1,500/mL, serum creatinine $\leq$ 1.5 mg/dl (or if > 1.5, a measured 24 hour creatinine clearance $\geq$ 50 mL/min), AST and ALT $\leq$ 2.5 × NL, and bilirubin $\leq$ 1.5 × NL (in patients with clinical evidence of Gilbert's disease, $\leq$ 3 × NL). Patients were also required to be $\geq$ 4 weeks from prior radiation or chemotherapy; > 2 weeks from hormonal therapy; and > 4 weeks from prior experimental therapy. Patients receiving agents that had major interactions with the CYP3A4 drug metabolizing system and that could not be discontinued were not allowed on study. Furthermore, patients with untreated brain metastases (or local treatment of brain metastases within the last 6 months) were excluded.

### Drug Supply and Treatment Schema

Tariquidar was supplied by Xenova Ltd., and docetaxel by the Warren G. Magnuson Clinical Center Pharmacy. This was an open-label pharmacokinetic/pharmacodynamic trial. To generate equivalent pharmacokinetic data, 40 mg/m$^2$ docetaxel was administered on both day 1 and 8 of cycle 1, and patients were randomized to receive tariquidar 150 mg on either day 1 or day 8 of cycle 1 (Supplemental Figure 1). Tariquidar was given intravenously over

40 minutes before initiation of the 1 hr docetaxel infusion. Tariquidar was administered alone on or about day 22 (week 4 of cycle 1) to allow sestamibi imaging, uncomplicated by docetaxel administration. From cycle 2 and onward, 75 mg/m$^2$ docetaxel was administered every 21 days in combination with a single 150 mg tariquidar dose. Growth factor support was allowed in cycles 2 and beyond, as clinically indicated. If the nadir ANC was ≥ 1000, the nadir platelet count was ≥ 50,000, and no grade 3/4 non-hematologic toxicities were observed after 75 mg/m$^2$ docetaxel, the dose could be increased to 90 mg/m$^2$ in subsequent cycles, provided no delay was required to start the next cycle.

## Pharmacodynamics

Pharmacokinetic and pharmacodynamic studies were performed in cycle 1, where docetaxel was administered on days 1 and 8. Measurement of Pgp-mediated rhodamine 123 transport in CD56+ cells was performed as described [20]. Whole blood was obtained from patients prior to treatment (pre), and 24 h and 48 h after the start of the tariquidar infusion. Rhodamine 123 (final concentration 0.5 μg/ml) was added to aliquots of blood in the presence or absence of 3 μg/ml of the Pgp inhibitor valspodar (PSC 833); one aliquot was incubated without rhodamine to assess auto-fluorescence. Aliquots were incubated for 30 min at 37°C after which mononuclear cells were separated by density gradient. Aliquots were then washed with cold PBS, divided and either held at 4°C or re-suspended in rhodamine-free complete medium (phenol red-free Richter's medium with 10% fetal calf serum) continuing with or without valspodar and allowed to incubate an additional 1h at 37°C. All aliquots were then washed and stained with phycoerythin-labeled anti-CD56 antibody (BD Biosciences, San José, CA) at 4°C. Multiparameter flow cytometry was conducted on a FACSort flow cytometer (BD Biosciences) equipped with an argon laser. Intracellular rhodamine fluorescence was calculated in CD56+ cells using the FlowJo analysis program (v 6.4.7, Tree Star Inc., Ashland OR).

A secondary objective of this study was to establish whether tariquidar (150 mg) modulates Pgp in tumors of patients. Evaluation was performed by [99mTc]-sestamibi (Cardiolyte) scanning in conjunction with a solitary tariquidar dose administered in the fourth week of cycle 1. A baseline [99mTc]-sestamibi scan was obtained before the administration of tariquidar. A minimum of 48 hours later, on or about day 22, a single dose of tariquidar was administered, followed by a second [99mTc]-sestamibi scan. Cycle 1 was considered complete at day 28; subsequent cycles were 21 days in duration.

## Pharmacokinetics

**Sample collection and analysis—**Blood samples were collected in tubes containing sodium heparin as an anticoagulant on days 1 and 8. Samples were obtained before administration, 1h after the start of the docetaxel infusion (several minutes prior to the end of infusion) and at 1 h 5 min, 1h 15 min, 1h 30 min, 1h 45 min, 3 h, 5 h, 7h, 12h, and 24h. Samples were centrifuged for 5 minutes at $1200 \times g$. The plasma supernatant was stored at -80 °C until analysis.

All samples were analyzed using an analytical assay validated for measurement of docetaxel in human plasma. Briefly, 100 μL of plasma was transferred to a glass centrifuge tube, and 1mL of methyl tert-butyl ether (MTBE) containing the internal standard, paclitaxel, was added. After vortex mixing and centrifugation, the supernatant layer was collected and evaporated. The residue was reconstituted with a mixture of methanol/0.1% formic acid (v:v 60:40), of which 5 μL solution was injected into the Acquity UPLC (Waters Corp, Milford, MA, USA). Mass analysis was achieved by a Quattro Permier Triple Quadrupole Mass Spectrometer (Waters Corp, Milford, MA, USA) using electrospray ionization. The compounds were separated on a Symmetry Shield Rp18 column (2.1× 50 mm, 3.5 μm) using

a mobile phase consisting of methanol (B)/0.1% formic acid (A) at a flow rate of 0.2 mL/min. Initial condition, 40% B was gradually increased to 65% within the first 4 min of gradient run, then held for 3 min before it was set to the initial condition. The total run time was 8 min. Two ion transitions were monitored: docetaxel, 808.5→527.3 *m/z*; and paclitaxel, 854.4→569.1, *m/z*. Assay range was 1 to 1000 ng/mL. Accuracy and precision of three concentrations of quality control samples ranged from 98% to 104.3% and 0 to 3.2%.

**Pharmacokinetic data analysis and statistics**—Non-compartmental pharmacokinetic data analysis was performed using WinNonLin, v.5.2. The maximum plasma concentration (Cmax) was the observed value. The area under the concentration-time curve (AUC) from time zero to 24 h after the start of the docetaxel infusion ($AUC_{0-24}$) was calculated using the linear trapezoidal method. Non-parametric statistical methods for analyzing data from two-period crossover trials were used [21]. Specifically, tests were first performed to determine if there was a period or carry-over effect (comparing day 1 and 8), and a residual effect, prior to testing whether there was a difference between docetaxel parameters when administered with and without tariquidar. As the parameters presented in this report did not exhibit a significant period effect, the difference in the parameter values for docetaxel with tariquidar minus those without tariquidar were determined by a Wilcoxon signed rank test. P-values less than 0.05 were considered to be statistically significant. For all data sets, geometric mean and 95% confidence interval (95% CI) were calculated using GraphPad Prism (La Jolla, CA).

## Results

### Patient Characteristics

Table 1 summarizes the tumor types, performance status, age and prior therapies of the 48 patients enrolled on the trial. The 3 main tumor types were ovarian (38%), cervical (29%) and lung (29%). A protocol amendment allowed inclusion of patients with renal cell carcinoma (RCC) who had previously been treated with either sunitinib or sorafenib and had been deemed ineligible for IL-2 therapy. Only 2 patients (4%) with RCC were enrolled prior to reaching the accrual ceiling of the patient population originally planned. All patients had an ECOG performance status score of 2 or better. All patients had received at least one prior cytotoxic chemotherapy regimen prior to commencing on study. The mean number of prior regimens was 4.8, and median 4. Approximately 50% of patients had received at least 3 prior regimens prior to enrollment and 29% had received ≥6 (range 6-16) prior treatments.

### Docetaxel/Tariquidar Dose Administered

All patients received 40 mg/ m$^2$ docetaxel on days 1 and 8, and 150 mg tariquidar randomized to either day 1 or day 8. This schedule was selected to allow detection of the effects of tariquidar on pharmacokinetics when only 8 days separated the two sampling periods, and using a dose of docetaxel that would be safe when repeated in a short interval. Though non-linearity cannot be excluded, it was not expected based on previously published data on docetaxel pharmacokinetics[22,23]. Cycle 2 commenced after completion of the pharmacokinetic and pharmacodynamic studies in cycle 1. In this and subsequent cycles, 75 mg/m$^2$ of docetaxel was administered in combination with a single 150 mg tariquidar dose. Granulocyte colony stimulating factor (GCSF) was allowable by the protocol after cycle 1 and it was used if clinically indicated based on toxicity or on prior history of pelvic irradiation. Doses were reduced per protocol for toxicity. Although 75mg/m$^2$ was considered an adequate dose, some patients had minimal to no toxicity and the protocol allowed dose increases. Among the 187 cycles administered in cycles 2 and beyond, 160 doses were administered at 75 mg/m$^2$ (86%), 11 doses at 60 mg/m$^2$ (6%), one dose at 40 mg/m$^2$ (<1%), 14 doses at 90 mg/m$^2$ (7%) and one dose at 100 mg/m$^2$ (<1%). A total number of 235 cycles

of tariquidar in combination with docetaxel were administered to 48 patients with a median of 4 cycles per patient, a mean of 4.9 cycles and a range of 1 to 26. Five subjects received more than 9 cycles and one received 26 cycles.

### Toxicities

One of the primary objectives of this study was to assess the safety and toxicity profile of the two-drug combination. In general, the combination was well tolerated. Two patients (4%) among the 48 receiving 40 mg/m$^2$ docetaxel in cycle 1 experienced grade 3 febrile neutropenia and received docetaxel dose reductions in cycle 2, to 60 mg/m$^2$ and 40 mg/m$^2$ respectively. One patient had received extensive prior pelvic radiotherapy and the other had extensive liver involvement with pre-existing liver dysfunction that became apparent after commencing on study. Table 2 outlines grade 3 or 4 toxicities seen during cycles 1 and 2 (n= 48 and 40, respectively). Ten percent of patients had grade 4 neutropenia in cycle 1, which increased to 48% in cycle 2. GCSF was frequently used in subsequent cycles; grade 3/4 neutropenia was observed in 41% of 126 cycles (cycles 2 – 6), as shown in Supplemental Table 1. The rates of grade 3 anemia and thrombocytopenia were relatively low, 8% and 2%, respectively. Non-hematologic toxicities overall were generally grade 1 or 2 with the exceptions being grade 3 fatigue (6%), hypoalbuminemia (4%), and hyponatremia (4%) (Supplemental Table 1). An uncommon toxicity observed in this study was docetaxel-induced epiphora secondary to canalicular stenosis. Fifteen patients (31%) developed epiphora, of which 10 were grade 1, 3 grade 2 and 2 were grade 3. No one discontinued therapy for epiphora; four patients required ophthalmological evaluation, and 3 were managed with bicanalicular silicone intubation or dacryocystorhinostomy to prevent stenosis.

### Pharmacodynamics

Since CD56+ peripheral blood mononuclear cells express high endogenous levels of Pgp, inhibition of Pgp-mediated rhodamine 123 efflux from CD56+ cells has been used to determine efficacy of Pgp inhibition in clinical trials[20,24]. As shown in Figure 1A, upper row, left panel, rhodamine 123 fluorescence was assessed in CD56+ cells from a patient after a 30 min loading period in the absence (solid line, Control histogram) or presence of exogenously added valspodar (dashed line, PSC histogram), which fully inhibits Pgp-mediated rhodamine transport in this assay. The remaining panels represent cells in which a 60 min efflux period followed, continuing the cells without or with exogenous valspodar (to generate Efflux and PSC/Efflux histograms). We obtained the difference between the Control and PSC histograms and the difference between the Efflux and PSC/Efflux histograms at each time-point for each patient (a representative set of assays is shown in the remaining panels of Figure 1A: prior to (Pre), or 24 h and 48 h after, the start of the tariquidar infusion). Overlap of Efflux and PSC/Efflux histograms reflects complete inhibition of Pgp by the tariquidar administered to the patient. Box-plots of the difference between Control and PSC histograms and Efflux and PSC/Efflux histograms in 41 patients are shown in Figures 1B and 1C, respectively. While rhodamine efflux from CD56+ cells was significantly decreased due to tariquidar administration at the 24 and 48 h time-points compared to Pre levels, inhibition appeared more variable at the 48 h time-point.

### 99mTc-Sestamibi accumulation

Sestamibi results were available in 35 (73%) of the 48 patients and were analyzed as previously described[13,14]. No statistically significant increase in exposure, measured as area under the concentration curve (AUC) up to three hours (AUC$_{0-3}$) was noted for cardiac or lung tissue (two-tailed Student's t-test). Figure 2 presents a box plot analysis of the sestamibi AUC monitored from 0 to 3 hours (AUC$_{0-3}$) in heart, lung, liver, and visible tumors in the presence or absence of tariquidar. A statistically significant change in AUC

was detected in both liver and visualized tumor tissue (both P<0.001). When the $AUC_{0-3}$ was evaluated as a percentage change and normalized to the $AUC_{0-3}$ of the heart ($nAUC_{0-3}$), an increased $nAUC_{0-3}$ for the liver was observed ranging from 5.8% to 252% over the pre-tariquidar scan. The median increase in liver uptake was 82.2%, while the median increase in visualized tumors was 12.4%, ranging from -7.2% to 24.1%. The results also demonstrated that actual liver $AUC_{0-3}$ was much larger than the $AUC_{0-3}$ of the tumors. Post-tariquidar liver $AUC_{0-3}$ ranged from 406 to 2094 min*cpm/px/mCi, whereas the $AUC_{0-3}$ of the tumor measured from 141 to 233 min*cpm/px/mCi.

Examining the lung cancer cohort, where 10 of 13 patients with lung cancer had visible lesions on sestamibi imaging, lung tumors in 8 of the 10 demonstrated an increased nAUC ranging from 12% to 24.1%. In addition to the 3 patients with lung masses on CT scan in whom no tumor sestamibi uptake could be identified, many patients demonstrated a mixed pattern with some lesions showing sestamibi uptake while others did not. Figure 3A shows a large supraclavicular mass on CT that demonstrates sestamibi uptake after tariquidar, while Figure 3B shows a sestamibi scan with mixed results in which a large peripheral right lung lesion is sestamibi negative. Supplemental Figure 2 demonstrates a composite graph of sestamibi uptake levels over time in a single patient in the liver, heart and left and right lung tumors pre and post tariquidar.

### Docetaxel Pharmacokinetics

Twenty-four hour pharmacokinetics were evaluable in a total of 45 patients, for a total of 76 cycles; 37 with tariquidar and 39 without. Thirty-one patients had evaluable pharmacokinetics on both C1D1 and C1D8, allowing for assessment of the effect of tariquidar on docetaxel disposition. A comparison of exposure ($AUC_{0-24}$ and Cmax) was performed. As shown in Supplementary Table 2, no significant difference in docetaxel disposition was observed based on pairwise comparison with and without tariquidar, though substantial inter-individual variability was observed. Variability can be seen in Figures 4A and 4B, which graphically display the pairwise comparison of these pharmacokinetic parameters. The docetaxel exposure ratios with and without tariquidar are shown in Figure 4C. The geometric mean ratios for docetaxel Cmax and AUC were 0.907 (95% CI: 0.697-1.18) and 1.07 (95% CI: 0.922-1.25). Similarly, no effect of sequence was observed, by comparison of docetaxel clearance when administered as a single agent on either C1D1 or C1D8, as shown in Figure 4D.

### Response Evaluation

In total, 4 partial responses (PR) were seen (8%). Three PRs measuring 40%, 57% and 67% reduction in tumor size by RECIST criteria were independently verified in patients with heavily pretreated non small cell lung cancer. One PR measuring 30% was seen in a patient with advanced ovarian cancer who had received 5 previous regimens. Although eleven (23%) patients had received prior docetaxel, none of the four patients with measurable response had received prior docetaxel. Sixteen patients demonstrated stable disease (33%) ranging from 13 weeks to 38 weeks. Stable disease as per RECIST criteria was attributed only after cycle 4 (12 weeks) of treatment. Of those with stable disease, 3 patients had evidence of prolonged clinical benefit of greater than 8 months lasting 32, 34 and 38 weeks respectively. Twenty patients (42%) had progressive disease and 8 patients (17%) were considered not evaluable. Among these, five patients refused to return for further therapy and restaging after receiving cycle 1. Three patients developed complicating disease or intercurrent illness and were withdrawn from the trial for medical reasons.

## Discussion

This report summarizes a pharmacodynamic study of docetaxel in combination with the Pgp inhibitor, tarquidar. We determined that a docetaxel dose of 75 mg/m$^2$ every 3 weeks can be safely administered with a single 150 mg dose of tariquidar. Pharmacodynamic studies confirmed complete inhibition of Pgp in circulating mononuclear cells. $^{99m}$Tc-sestamibi was used as a surrogate to evaluate drug accumulation in normal and tumor tissue and confirmed increased accumulation in liver and in a subset of tumors. No significant difference in docetaxel disposition was observed based on pairwise comparison with and without tariquidar. However, pharmacogenetic studies are currently underway to elucidate the cause of the inter-individual and intra-individual variability observed. Although not a primary endpoint, clinical benefit was noted in a number of patients, including partial remissions in four tumors (3 NSCLC and 1 ovarian carcinoma).

The toxicities seen in this study were acceptable and were usual for the side effects seen with docetaxel. Since this was a heavily pretreated patient population, GCSF was used to support granulocyte counts, such that although grade 3/4 neutropenia was observed in 41% of 126 cycles, only 6 episodes of febrile neutropenia were reported. At present there is no evidence to suggest that Pgp inhibition via tariquidar in normal tissues leads to enhanced toxicity. Possibly the only toxicity observed that may have been related to the use of docetaxel in combination with tariquidar was epiphora secondary to canalicular stenosis. This is a recognized, but relatively rare side effect of taxane therapy that is seen more commonly in patients who receive weekly docetaxel (33-50%) than in those receiving three weekly docetaxel where it has been reported as conjunctivitis (11%)[25-27]. Thus, these data suggest that a therapeutic window does exist to improve tumor tissue uptake without increased toxicity due to increased uptake in normal cells, particularly in bone marrow cells.

An issue that is still not proven is whether Pgp inhibition can actually increase concentrations of anticancer agents in tumor tissue in the clinical setting. Inhibition of rhodamine efflux in circulating CD56$^+$ cells is a surrogate for Pgp inhibition in normal cells. As shown in Figure 1, CD56$^+$ cells from all patients demonstrated retention of rhodamine 24 hr after IV dosing of tariquidar with persistence to 48 hr in most. This is consistent with prior studies showing retention of rhodamine in CD56$^+$ cells following the inhibitors valspodar, tariquidar, or CBT-1[14,20,28,29]. However, the major limitation of the CD56$^+$ assay is that it reflects Pgp inhibition in the blood and not in the tumor.

As a strategy to evaluate Pgp inhibition in normal and tumor tissue, imaging with the radionuclide cardiac imaging agent $^{99m}$Tc-sestamibi was included in this study. This γ-emitting organo-technetium complex is a substrate for the Pgp efflux pump[30,31]. Cardiac tissue does not significantly express Pgp and therefore tends to accumulate and retain sestamibi. In tissues that express Pgp, such as the liver, kidney, and some tumors, retention of sestamibi increases in the presence of Pgp antagonists[13]. Similar results have been observed with another radiotracer, $^{99m}$Tc-tetrofosmin, which is also FDA approved for cardiac imaging. In lung cancer, radiotracer uptake has been correlated with response to treatment in small, single institution analyses, where striking inter-individual differences in $^{99m}$Tc-sestamibi or $^{99m}$Tc-tetrofosmin uptake were reported with absence of imaging uptake indicative of poor response to chemotherapy [32-38]. A recent meta-analysis concluded that $^{99m}$Tc-sestamibi scanning, particularly the initial uptake, can be used as a pre-selection technique to differentiate likely chemotherapy responders[38]. Although our baseline sestamibi studies do show striking differences between patients, there were not enough patients in the lung cancer subset to evaluate correlation between sestamibi imaging and response.

Apart from basal uptake, our study queried whether sestamibi retention was higher after tariquidar. Sestamibi results were available in 35 of the 48 patients, and an increased nAUC for the liver was noted, ranging from 5.8% to 252% after tariquidar. A modest although statistically significant 12% to 24% increase in sestamibi uptake was noted in visible lesions in 8 of 10 patients with lung cancer. We have previously recognized that quantitation by planar sestamibi imaging tends to record greater changes in AUC values for hepatic tissue than for tumor tissue[13]. A previous study noted increases in $nAUC_{0-3}$ from -14 to +278% in liver and from 36 to 263% in tumors of 8 patients among 17 who had imageable tumors, with the most pronounced effects in patients with renal or adrenocortical cancer, both tumor types with known high expression of Pgp[13]. High Pgp expression may explain the relatively better results in the prior study and in liver tissue, compared to lung tumors. Alternatively, Pgp may not be the most important arbiter of sestamibi accumulation in lung cancer. Since sestamibi is a substrate of both Pgp and MRP1 transporters[39], it is tempting to conclude that the lack of a convincing tariquidar effect in the lung tumors in our patients is due to the confounding effect of another transporter, such as MRP1, with documented expression in lung cancer[40]. The lack of effect of tariquidar on sestamibi retention could be explained by the presence of other transporters, including other ABC transporters and also organic anion transporting polypeptides (OATPs) that have been shown to modulate chemotherapeutic concentrations. Notably, tariquidar does not inhibit MRP1[41] and ABCG2 has been shown not to transport sestamibi[42].

Another explanation for the lesser changes seen in tumor tissue compared to the liver is that with planar imaging, the counts per pixel over a region of interest include all counts in that region coming from tissue lying along the axis perpendicular to the face of the gamma camera (ventral-dorsal), as well as scatter from surrounding pixels. When the liver is imaged, a large number of counts along this axis come from liver tissue as compared to the lung tumors visualized in this study, which usually only extended a few centimeters in any direction -- thus, many of the counts in our tumor regions of interest (ROIs) actually represented lung or other normal tissue. Secondly, scatter from surrounding pixels is usually greater in liver than that in tumor because of its size and high sestamibi uptake compared to tumors that are relatively smaller and have lower uptake of sestamibi. Tomographic imaging with attenuation correction should eliminate much of this problem, and we are currently exploring this using $^{94m}Tc$-sestamibi PET imaging.

A number of studies have addressed the question of whether Pgp expression in lung cancer is a determinant of clinical outcome. While there is evidence that *MDR-1* expression may correlate with outcome, particularly in SCLC[40,43,44], for NSCLC, both poor outcome[43,45] and no impact on outcome[46,47] have been reported. More recent studies have examined the effect of other ABC transporters such as MRP1 or ABCG2 (BCRP) and conflicting conclusions suggesting both poor outcome and no impact on outcome have been reported[47-49]. Little work has been done examining the expression of other ABC transporters. One unique feature of tariquidar is that it has been shown to inhibit both Pgp- and ABCG2-mediated resistance *in vitro*, although higher concentrations are required to inhibit ABCG2. As there are no clinical surrogates for inhibition of ABCG2, it is unclear whether clinically achievable tariquidar levels would inhibit ABCG2 activity in tumors. The variable uptake of sestamibi in tumor tissue, and the failure of tariquidar to make a dramatic difference, suggests that both functional studies assessing drug accumulation and studies characterizing transporters that affect drug concentrations are needed in lung cancer.

Although four patients with heavily pretreated cancer attained partial responses, this trial was not designed to answer the question of whether Pgp inhibition provided clinical benefit —experience with Pgp inhibition trials to date has clearly shown that randomized designs are necessary to answer this question. Two double-blind, randomized, placebo-controlled,

multicenter, phase III studies in advanced non small cell lung cancer combining tariquidar with carboplatin/paclitaxel or with vinorelbine closed early due to toxicity. This was ascribed to the combination of high dose chemotherapeutics in a lung cancer population, with a pharmacodynamic effect on the bone marrow, rather than a pharmacokinetic interaction[50]. Thus the questions of whether drug accumulation could be increased in lung cancer or whether there could be an added clinical value in lung cancer were not answered.

We are now in the era of utilizing predictive and prognostic biomarkers to individualize patient therapy, and it is clear that drug resistance is too complex to be attributed to a single protein. Where it has been evaluated, tumor drug accumulation is far more variable than generally assumed. Imaging agents or other strategies are required to identify tumors in which drug accumulation is a critical determinant of treatment response. This trial highlights the need to determine whether Pgp, or other transporters such as MRP1 or ABCG2, or the OATPs, play a dominant role in drug uptake in clinical tumors. With the increasing number of novel targeted agents recognized as substrates for Pgp or ABCG2-mediated efflux (imatinib, dasatinib, nilotinib, lapatinib, and sunitinib have all been shown to interact with these transporters), there is new impetus to answer this question. If we are to deliver personalized medicine, we need to know that drugs are penetrating into tumor tissue. Improved imaging modalities need to be developed so that they can be coupled with novel therapeutics. A functional imaging study with greater sensitivity than sestamibi, as shown in this study, could be used to aid in choosing between available therapeutics. As molecular profiling of patients tumors and delivering personalized therapies becomes the norm it is clear that an improved understanding of the factors that affect drug accumulation in human cancer will be needed to deliver on the promise of exciting novel therapies.

## Supplementary Material

Refer to Web version on PubMed Central for supplementary material.

## Acknowledgments

## References

1. Fojo A, Akiyama S, Gottesman MM, Pastan I. Reduced drug accumulation in multiply drug-resistant human KB carcinoma cell lines. Cancer Res. 1985; 45:3002–7. [PubMed: 4005839]

2. Gottesman MM, Fojo T, Bates SE. Multidrug resistance in cancer: role of ATP-dependent transporters. Nat Rev Cancer. 2002; 2:48–58. [PubMed: 11902585]

3. Leonard GD, Fojo T, Bates SE. The role of ABC transporters in clinical practice. Oncologist. 2003; 8:411–24. [PubMed: 14530494]

4. Rowinsky EK, Smith L, Wang YM, et al. Phase I and pharmacokinetic study of paclitaxel in combination with biricodar, a novel agent that reverses multidrug resistance conferred by overexpression of both MDR1 and MRP. J Clin Oncol. 1998; 16:2964–76. [PubMed: 9738565]

5. Hyafil F, Vergely C, Du Vignaud P, Grand-Perret T. In vitro and in vivo reversal of multidrug resistance by GF120918, an acridonecarboxamide derivative. Cancer Res. 1993; 53:4595–602. [PubMed: 8402633]

6. Keller RP, Altermatt HJ, Nooter K, et al. SDZ PSC 833, a non-immunosuppressive cyclosporine: its potency in overcoming P-glycoprotein-mediated multidrug resistance of murine leukemia. Int J Cancer. 1992; 50:593–7. [PubMed: 1347037]

7. Seiden MV, Swenerton KD, Matulonis U, et al. A phase II study of the MDR inhibitor biricodar (INCEL, VX-710) and paclitaxel in women with advanced ovarian cancer refractory to paclitaxel therapy. Gynecol Oncol. 2002; 86:302–10. [PubMed: 12217752]

8. Fracasso PM, Brady MF, Moore DH, et al. Phase II study of paclitaxel and valspodar (PSC 833) in refractory ovarian carcinoma: a gynecologic oncology group study. J Clin Oncol. 2001; 19:2975–82. [PubMed: 11408492]

9. Chico I, Kang MH, Bergan R, et al. Phase I study of infusional paclitaxel in combination with the P-glycoprotein antagonist PSC 833. J Clin Oncol. 2001; 19:832–42. [PubMed: 11157037]

10. Massey, PRFT.; Bates, SE. ABC Transporters: Involvement in multidrug resistance and drug disposition.. In: Figg, WD.; McLeod, HL.; Chau, CH.; Rudek, MA., editors. Handbook of Anticancer Pharmacokinetics and Pharmacodynamics. 2nd Edition. Springer Science+Business Media, LLC; New York: 2011.

11. Martin C, Berridge G, Mistry P, Higgins C, Charlton P, Callaghan R. The molecular interaction of the high affinity reversal agent XR9576 with P-glycoprotein. Br J Pharmacol. 1999; 128:403–11. [PubMed: 10510451]

12. Stewart A, Steiner J, Mellows G, Laguda B, Norris D, Bevan P. Phase I trial of XR9576 in healthy volunteers demonstrates modulation of P-glycoprotein in CD56+ lymphocytes after oral and intravenous administration. Clin Cancer Res. 2000; 6:4186–91. [PubMed: 11106230]

13. Agrawal M, Abraham J, Balis FM, et al. Increased 99mTc-sestamibi accumulation in normal liver and drug-resistant tumors after the administration of the glycoprotein inhibitor, XR9576. Clin Cancer Res. 2003; 9:650–6. [PubMed: 12576431]

14. Abraham J, Edgerly M, Wilson R, et al. A phase I study of the P-glycoprotein antagonist tariquidar in combination with vinorelbine. Clin Cancer Res. 2009; 15:3574–82. [PubMed: 19417029]

15. Mistry P, Stewart AJ, Dangerfield W, et al. In vitro and in vivo reversal of P-glycoprotein-mediated multidrug resistance by a novel potent modulator, XR9576. Cancer Res. 2001; 61:749–58. [PubMed: 11212278]

16. Pusztai L, Wagner P, Ibrahim N, et al. Phase II study of tariquidar, a selective P-glycoprotein inhibitor, in patients with chemotherapy-resistant, advanced breast carcinoma. Cancer. 2005; 104:682–91. [PubMed: 15986399]

17. Boniface G FD, Atsmon J, Inbar M, Van Tellingen O, Abraham J, Bates S, Fojo T, Thomas H, Mould G, Steiner J, Mellows G. XR9576 (tariquidar), a potent and specific P-glycoprotein inhibitor, has minimal effects on the pharmacokinetics of paclitaxel, doxorubicin, and vinorelbine and can be administered with full-dose chemotherapy in patients with cancer. . ASCO Proceedings. 2002

18. Chan S, Friedrichs K, Noel D, et al. Prospective randomized trial of docetaxel versus doxorubicin in patients with metastatic breast cancer. J Clin Oncol. 1999; 17:2341–54. [PubMed: 10561296]

19. Catimel G, Verweij J, Mattijssen V, et al. Docetaxel (Taxotere): an active drug for the treatment of patients with advanced squamous cell carcinoma of the head and neck. EORTC Early Clinical Trials Group. Ann Oncol. 1994; 5:533–7. [PubMed: 7918125]

20. Robey R, Bakke S, Stein W, et al. Efflux of rhodamine from CD56+ cells as a surrogate marker for reversal of P-glycoprotein-mediated drug efflux by PSC 833. Blood. 1999; 93:306–14. [PubMed: 9864175]

21. Koch G. The use of non-parametric methods in the statistical analysis of the two-period change-over design. Biometrics. 1972; 28:577–84. [PubMed: 4556704]

22. McLeod HL, Kearns CM, Kuhn JG, Bruno R. Evaluation of the linearity of docetaxel pharmacokinetics. Cancer Chemother Pharmacol. 1998; 42:155–9. [PubMed: 9654116]

23. Goncalves A, Viret F, Ciccolini J, et al. Phase I and pharmacokinetic study of escalating dose of docetaxel administered with granulocyte colony-stimulating factor support in adult advanced solid tumors. Clin Cancer Res. 2003; 9:102–8. [PubMed: 12538457]

24. Witherspoon SM, Emerson DL, Kerr BM, Lloyd TL, Dalton WS, Wissel PS. Flow cytometric assay of modulation of P-glycoprotein function in whole blood by the multidrug resistance inhibitor GG918. Clin Cancer Res. 1996; 2:7–12. [PubMed: 9816083]

25. Tsalic M, Gilboa M, Visel B, Miller B, Haim N. Epiphora (excessive tearing) and other ocular manifestations related to weekly docetaxel: underestimated dose-limiting toxicity. Med Oncol. 2006; 23:57–61. [PubMed: 16645230]

26. Burstein HJ, Manola J, Younger J, et al. Docetaxel administered on a weekly basis for metastatic breast cancer. J Clin Oncol. 2000; 18:1212–9. [PubMed: 10715290]

27. Valero V, Holmes FA, Walters RS, et al. Phase II trial of docetaxel: a new, highly effective antineoplastic agent in the management of patients with anthracycline-resistant metastatic breast cancer. J Clin Oncol. 1995; 13:2886–94. [PubMed: 8523051]

28. Robey RW, Shukla S, Finley EM, et al. Inhibition of P-glycoprotein (ABCB1)- and multidrug resistance-associated protein 1 (ABCC1)-mediated transport by the orally administered inhibitor, CBT-1((R)). Biochem Pharmacol. 2008; 75:1302–12. [PubMed: 18234154]

29. Bates SE, Bakke S, Kang M, et al. A phase I/II study of infusional vinblastine with the P-glycoprotein antagonist valspodar (PSC 833) in renal cell carcinoma. Clin Cancer Res. 2004; 10:4724–33. [PubMed: 15269145]

30. Chen CC, Meadows B, Regis J, et al. Detection of in vivo P-glycoprotein inhibition by PSC 833 using Tc-99m sestamibi. Clin Cancer Res. 1997; 3:545–52. [PubMed: 9815718]

31. Bakker M, van der Graaf WT, Piers DA, et al. 99mTc-Sestamibi scanning with SDZ PSC 833 as a functional detection method for resistance modulation in patients with solid tumours. Anticancer Res. 1999; 19:2349–53. [PubMed: 10472354]

32. Ceriani L, Giovanella L, Bandera M, Beghe B, Ortelli M, Roncari G. Semi-quantitative assessment of 99Tcm-sestamibi uptake in lung cancer: relationship with clinical response to chemotherapy. Nucl Med Commun. 1997; 18:1087–97. [PubMed: 9423210]

33. Nishiyama Y, Yamamoto Y, Satoh K, et al. Comparative study of Tc-99m MIBI and TI-201 SPECT in predicting chemotherapeutic response in non-small-cell lung cancer. Clin Nucl Med. 2000; 25:364–9. [PubMed: 10795697]

34. Yüksel M, Cermik T, Doğanay L, et al. 99mTc-MIBI SPET in non-small cell lung cancer in relationship with Pgp and prognosis. Eur J Nucl Med Mol Imaging. 2002; 29:876–81. [PubMed: 12111127]

35. Komori T, Narabayashi I, Matsui R, Sueyoshi K, Aratani T, Utsunomiya K. Technetium-99m MIBI single photon emission computed tomography as an indicator of prognosis for patients with lung cancer-preliminaly report. Ann Nucl Med. 2000; 14:415–20. [PubMed: 11210093]

36. Fuster D, Vinolas N, Mallafre C, Pavia J, Martin F, Pons F. Tetrofosmin as predictors of tumour response. Q J Nucl Med. 2003; 47:58–62. [PubMed: 12714956]

37. Shih C, Shiau Y, Wang J, Ho S, Kao A. Using technetium-99m tetrofosmin chest imaging to predict taxol-based chemotherapy response in non-small cell lung cancer but not related to lung resistance protein expression. Lung. 2003; 181:103–11. [PubMed: 12953149]

38. Mohan HK, Miles KA. Cost-effectiveness of 99mTc-sestamibi in predicting response to chemotherapy in patients with lung cancer: systematic review and meta-analysis. J Nucl Med. 2009; 50:376–81. [PubMed: 19223414]

39. Gomes CM, Abrunhosa AJ, Pauwels EK, Botelho MF. P-glycoprotein versus MRP1 on transport kinetics of cationic lipophilic substrates: a comparative study using [99mTc]sestamibi and [99mTc]tetrofosmin. Cancer Biother Radiopharm. 2009; 24:215–27. [PubMed: 19409044]

40. Stewart DJ. Tumor and host factors that may limit efficacy of chemotherapy in non-small cell and small cell lung cancer. Crit Rev Oncol Hematol.

41. Pajeva IK, Wiese M. Structure-activity relationships of tariquidar analogs as multidrug resistance modulators. AAPS J. 2009; 11:435–44. [PubMed: 19504188]

42. Chen WS, Luker KE, Dahlheimer JL, Pica CM, Luker GD, Piwnica-Worms D. Effects of MDR1 and MDR3 P-glycoproteins, MRP1, and BCRP/MXR/ABCP on the transport of (99m)Tc-tetrofosmin. Biochem Pharmacol. 2000; 60:413–26. [PubMed: 10856437]

43. Kawasaki M, Nakanishi Y, Kuwano K, Takayama K, Kiyohara C, Hara N. Immunohistochemically detected p53 and P-glycoprotein predict the response to chemotherapy in lung cancer. Eur J Cancer. 1998; 34:1352–7. [PubMed: 9849416]

44. Kao A, Shiun SC, Hsu NY, Sun SS, Lee CC, Lin CC. Technetium-99m methoxyisobutylisonitrile chest imaging for small-cell lung cancer. Relationship to chemotherapy response (six courses of combination of cisplatin and etoposide) and pglycoprotein or multidrug resistance related protein expression. Ann Oncol. 2001; 12:1561–6. [PubMed: 11822755]

45. Yeh JJ, Hsu WH, Wang JJ, Ho ST, Kao A. Predicting chemotherapy response to paclitaxel-based therapy in advanced non-small-cell lung cancer with P-glycoprotein expression. Respiration. 2003; 70:32–5. [PubMed: 12584388]

46. Haque AK, Adegboyega P, Al-Salameh A, Vrazel DP, Zwischenberger J. p53 and P-glycoprotein expression do not correlate with survival in nonsmall cell lung cancer: a long-term study and literature review. Mod Pathol. 1999; 12:1158–66. [PubMed: 10619270]

47. Yoh K, Ishii G, Yokose T, et al. Breast cancer resistance protein impacts clinical outcome in platinum-based chemotherapy for advanced non-small cell lung cancer. Clin Cancer Res. 2004; 10:1691–7. [PubMed: 15014021]

48. Filipits M, Haddad V, Schmid K, et al. Multidrug resistance proteins do not predict benefit of adjuvant chemotherapy in patients with completely resected non-small cell lung cancer: International Adjuvant Lung Cancer Trial Biologic Program. Clin Cancer Res. 2007; 13:3892–8. [PubMed: 17606722]

49. Li J, Li ZN, Du YJ, Li XQ, Bao QL, Chen P. Expression of MRP1, BCRP, LRP, and ERCC1 in advanced non-small-cell lung cancer: correlation with response to chemotherapy and survival. Clin Lung Cancer. 2009; 10:414–21. [PubMed: 19900859]

50. Nobili S, Landini I, Giglioni B, Mini E. Pharmacological strategies for overcoming multidrug resistance. Curr Drug Targets. 2006; 7:861–79. [PubMed: 16842217]
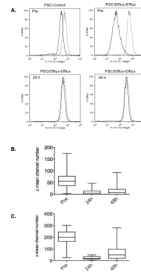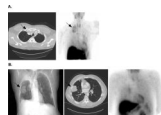
**Figure 1.**
Rhodamine efflux from CD56+ cells showing the extent and duration of Pgp inhibition. A) Whole blood was obtained from patients before tariquidar treatment (Pre) and at 24 and 48 h post treatment. Rhodamine fluorescence was measured in the CD56+ population. The blood was incubated with rhodamine 123 in the presence (Control histogram, solid line) or absence (PSC histogram, dashed line) of the Pgp inhibitor valspodar for 30 min (upper left panel). These samples were divided and a portion incubated in rhodamine-free medium for an additional hour, continuing with (PSC/Efflux histogram, dashed line) or without (Efflux histogram, solid line) valspodar. Representative histograms following this efflux period in Pre, 24, and 48 h samples are shown for an individual patient. For all patients, the difference in mean channel number between the PSC and Control histograms (B) or between the PSC/ Efflux and Efflux histograms (C) was calculated and compared by boxplot at each timepoint. The top and bottom of the boxes represent the 25th to 75th percentile, respectively, of the data, while the whiskers represent the minimum and maximum of all data.
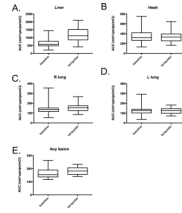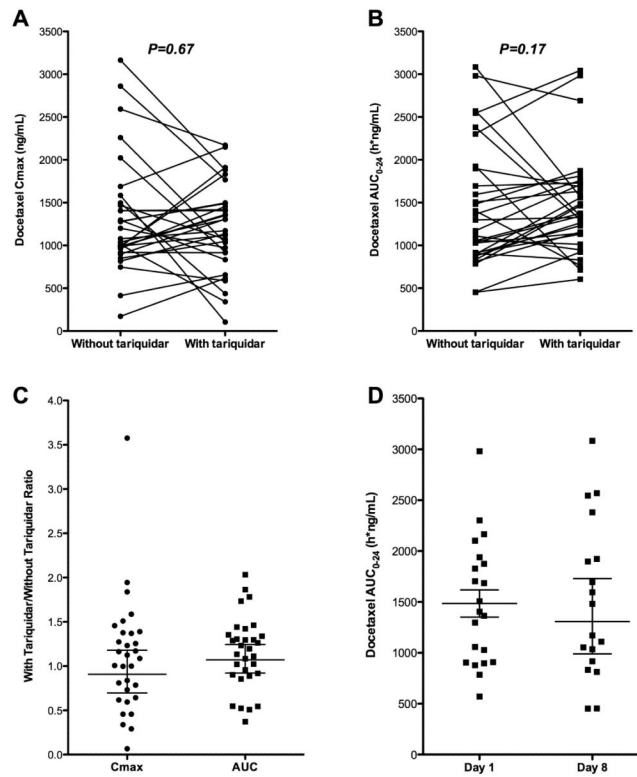
**Figure 2.**
Comparison of $^{99m}$Tc-Sestamibi areas under the concentration curve (AUC) before and after tariquidar administration. Boxplots of AUC before tariquidar and up to three hours after (AUC$_{0-3}$) for (A) liver, (B) heart (C) R lung, (D) L lung or (E) any lesion are shown. The box plots represent the calculated AUC$_{0-3h}$ mean not normalized to heart, with the top and bottom of the boxes representing the 25th to 75th percentile, respectively, of sestamibi counts obtained in radionuclide imaging. The whiskers represent the minimum and maximum of all data. A statistically significant difference in AUC after tariquidar was found in both liver and visualized tumor tissue (P<0.001).

**Figure 3.**
$^{99m}$Tc-Sestamibi scans performed in two patients with NSCLC. A: CT scan (left image) shows a large supraclavicular mass (denoted by arrow) that also exhibits $^{99m}$Tc-Sestamibi uptake (arrow, left image). B: Chest X-ray (left image) and CT scan (center image) clearly show a peripheral right lung lesion (denoted by arrow) that does not uptake $^{99m}$Tc-Sestamibi (right image).

**Figure 4.**
Changes in docetaxel pharmacokinetics when administered with or without tariquidar. A) Pairwise comparison of maximal docetaxel plasma concentration (Cmax) when administered with and without tariquidar. Each dot represents a single patient and cycle and lines connect the two cycles per patient. B) Pairwise comparison of docetaxel exposure ($AUC_{0-24}$) with and without tariquidar. C) Docetaxel exposure ratios of Cmax and $AUC_{0-24}$ calculated as (with tariquidar/without tariquidar). Each dot represents an individual patient. Horizontal lines represent the geometric mean and 95% CI. D) Docetaxel $AUC_{0-24}$ after single agent treatment did not differ based on sequence, based on comparison of docetaxel alone cycle on either Day 1 or Day 8. Each dot represents an individual patient. Horizontal lines represent the geometric mean and 95% CI.

**Table 1**

Clinical Characteristics of Patients (N=48)

| Characteristic | Number of Patients (%) |
|---|---|
| Histology | |
|    Ovarian cancer | 18 (38%) |
|    Lung cancer | 14 (29%) |
|    Cervical cancer | 14 (29%) |
|    Renal cancer | 2 (4%) |
| ECOG performance status | |
|    PS 0 | 7 (14.5%) |
|    PS 1 | 34 (71%) |
|    PS 2 | 7 (14.5%) |
| Age | |
|    18-30 years | 1 (2%) |
|    31-50 years | 20 (42%) |
|    51-80 years | 27 (56%) |
| No. of prior regimens | |
| 0 | 0 (0%) |
| 1 | 6 (13%) |
| 2 | 6 (13%) |
| 3 | 11 (23%) |
| 4 | 6 (13%) |
| 5 | 5 (10%) |
| ≥6 (range 6-16) | 14 (28%) |
| Prior chemotherapy | |
|    Taxane (Docetaxel/Paclitaxel) | 35 (73%) |
|    Platinum (Cisplatin/Carboplatin) | 44 (92%) |
|    Anthracycline | 17 (35%) |

**Table 2**

All Grade 3 and 4 Toxicities Occurring During Cycles 1 and 2

| Adverse event Hematological | Cycle 1 (n=48) | | Cycle 2 (n=40) | |
|---|---|---|---|---|
| | Grade 3 | Grade 4 | Grade 3 | Grade 4 |
| Leukopenia | 4 (8%) | 5 (10%) | 15 (38%) | 8 (20%) |
| Neutropenia | | 5 (10%) | 7 (18%) | 19 (48%) |
| Anemia | 3 (6%) | 1 (2%) | 5 (13%) | |
| Lymphopenia | 5 (10%) | | 1 (3%) | |
| Febrile Neutropenia | 2 (4%) | | 3 (8%) | |
| Thrombocytopenia | | 1 (2%) | | |

| Non Hematological | Grade 3 | Grade 4 | Grade 3 | Grade 4 |
|---|---|---|---|---|
| Hyponatremia | 2 (4%) | | 3 (8%) | |
| Fatigue | 1 (2%) | 1 (2%) | 2 (5%) | |
| Fever | 2 (4%) | | 2 (5%) | |
| Hypoalbuminemia | 2 (4%) | | 1 (3%) | |
| Epiphora | | | 1 (3%) | |
| Hyperglycemia | 1 (2%) | | 1 (3%) | |
| Hypokalemia | 2 (4%) | | | |
| Anorexia | | | | 1 (3%) |
| Diarrhea | | | 1 (3%) | |
| Constipation | | | 1 (3%) | |
| Hyperuricemia | | | | 1 (3%) |
| Thrombosis | | | | 1 (3%) |
| Arthalgia | 1 (2%) | | | |
| Dyspnea | 1 (2%) | | | |
| Hypophosphatemia | 1 (2%) | | | |

The toxicity reporting window included the entire 28 days of cycle 1